

Near-UV photo-induced modification in isorecticular metal–organic frameworks†

Corinne A. Allen and Seth M. Cohen*

Received 13th October 2011, Accepted 25th November 2011

DOI: 10.1039/c2jm15183a

A series of isorecticular metal–organic frameworks (IRMOFs) have been prepared using two different ligands protected with photolabile groups: 2-((2-nitrobenzyl)oxy)terephthalic acid (L1) and 2-((4,5-dimethoxy-2-nitrobenzyl)oxy)terephthalic acid (L2). Irradiation at either 365 or 400 nm results in postsynthetic deprotection (PSD), removing the nitrobenzyl protecting groups from these ligands and generating phenolic groups in the pores of the MOF (55–83% yield). The photochemical behaviour of the ligands in the IRMOFs was not wholly predicted by their reactivity in solution (*i.e.* free ligand). A mixed ligand approach was used, by combining L1 or L2 with NH₂-BDC to produce mixed ligand IRMOFs with 30–40% incorporation of the NH₂-BDC. These mixed-ligand IRMOFs were then subjected to both postsynthetic modification (PSM) and PSD. Two routes to achieve both PSM and PSD were explored: PSM followed by PSD (route 1) and PSD followed by PSM (route 2). When using 365 nm light for the PSD reaction, route 1 was superior due to absorption of NH₂-BDC at 365 nm. Irradiation at 400 nm gave fewer differences between route 1 and route 2, but the PSD reaction was less efficient (30–40%) for all systems. By combining PSD and PSM, MOFs with highly functionalized pores can be obtained through a combination of pre- and postsynthetic methods.

Introduction

Metal–organic frameworks (MOFs) are an intriguing class of hybrid materials that have been extensively studied in recent years.^{1–3} Also known as porous coordination polymers (PCPs) they are comprised of metal ions linked by organic molecules and are of interest due to their structured, porous, and highly tunable nature. Since the introduction of MOFs, many groups have sought to make functionalized, and therefore specially tailored, materials. With thousands of organic transformations available, the challenge remains of how to apply these reactions to MOFs while maintaining their structural integrity. It has been established that functionality can be directly incorporated into a MOF by simply using a functionalized organic linker molecule.⁴ However, this method is limited to functional groups that will not interfere with MOF formation. Based on the idea that a chemical ‘handle’ or ‘tag’ can be introduced in a ‘presynthetic’ fashion, the addition of functional groups after framework formation *via* these handles has been termed ‘postsynthetic modification’ (PSM).^{5–7} The PSM method has produced materials that would otherwise remain difficult or impossible to prepare by presynthetic approaches.⁸ Recently, Hupp,⁹

Telfer,^{10,11} and Cohen¹² introduced a related strategy that has been coined ‘postsynthetic deprotection’ (PSD). PSD involves synthesizing the framework with a protected functional group on the linker, then using suitable stimuli (*e.g.* heat, light, chemical, *etc.*) to remove the protecting group, revealing the desired functionality.¹¹

Multifunctional or ‘multivariate’ materials¹³ have been realized using mixed-ligand strategies and various combinations of pre- and postsynthetic approaches.^{13–18} Using a combination of these methods can lead to highly functionalized materials without complicating the synthetic conditions required to obtain the desired MOF. Within this theme of multiple modification methods, here we report the use of a light-activated PSD reaction in combination with a PSM reaction to generate functionalized isorecticular metal–organic frameworks (IRMOFs).

Utilizing light as a mild and efficient stimulus for chemical transformations has been studied on a multitude of platforms, including MOFs.^{19–23} Previously, we showed 2-nitrobenzyl protecting groups could be used to reveal pendant phenol and catechol groups in a UCMC-1 (University of Michigan Crystalline Materials) lattice.¹² 2-Nitrobenzyl derivatives are photolabile protecting groups that are commonly used to protect alcohols, esters, amides, and amines and are easily released upon exposure to near-UV light. Despite these and other studies of photochemistry in MOFs, there are no reports that compare the behaviour of photolabile groups in a framework *versus* in solution. There is precedence for the MOF to modify solution state

Department of Chemistry and Biochemistry, University of California, San Diego, La Jolla, California, 92093-0358, United States. E-mail: scohen@ucsd.edu; Fax: +1-858-822-5598; Tel: +1-858-822-5596

† Electronic Supplementary Information (ESI) available: Fig. S1–S9, Tables S1–S4. See DOI: 10.1039/c2jm15183a

behaviour as seen by Champness and George when monitoring charge transfer bands.²⁴ Here, two different photolabile protecting groups were incorporated into the IRMOF lattice and their photocleavage at two different wavelengths was investigated (Scheme 1). Additionally, these ligands were incorporated into mixed-ligand IRMOFs that were subjected to tandem PSM/PSD for functionalization. We find that successful execution of the light-triggered PSD reaction is dependent on order in which the PSD and PSM reactions are performed.

Experimental

General

N,N-Diethylformamide (DEF) was purchased from TCI America. Zinc nitrate hexahydrate (98%) and *N,N*-dimethylformamide (DMF) was purchased from Sigma-Aldrich Inc. 4,5-Dimethoxy-2-nitrobenzyl bromide (97%) was purchased from Acros Organics. All chemicals were used without further purification. ¹H NMR spectra were recorded on a Varian FT-NMR spectrometer (400 MHz). ESI-MS was performed using a Thermo-Finnigan LCQ-DECA mass spectrometer and analyzed using the Xcalibur software suite. Thermogravimetric analysis was done using a TA instrument Q600 SDT instrument. Powder X-ray diffraction spectra were collected on a Bruker D8 Advance diffractometer at 40 kV, 40 mA for Cu K α ($\lambda = 1.5417 \text{ \AA}$). Gas sorption measurements were performed on a Micromeritics ASAP 2020 Adsorption Analyzer. Surface areas were calculated using the Brunauer-Emmett-Teller (BET) method. All reported BET values have a standard deviation of approximately $\pm 150 \text{ m}^2 \text{ g}^{-1}$ based on at least three independent experiments. Single crystal X-ray diffraction data was collected at 200 K on a Bruker Apex diffractometer using Mo K α radiation ($\lambda = 0.71073 \text{ \AA}$) with the Apex 2010 software. Solid State UV-Vis absorbance spectra were taken on a StellarNetEPP 2000C spectrometer with a diffuse reflectance probe. Solution UV-Vis absorbance spectra

were collected on a Perkin-Elmer Lambda 25 UV-Vis spectrophotometer.

Ligands

L1 was synthesized as previously reported.¹² L2 was synthesized following a related procedure (ESI).[†]

IRMOFs

2-((2-Nitrobenzyl)oxy)terephthalic acid (L1, 317 mg, 1 mmol) or 2-((4,5-dimethoxy-2-nitrobenzyl)oxy)terephthalic acid (L2, 377 mg, 1 mmol) and $\text{Zn}(\text{NO}_3)_2 \cdot 6\text{H}_2\text{O}$ (832 mg, 2.8 mmol) were dissolved in DMF for L1 or DEF for L2 (50 mL). This was divided into 10 mL portions and transferred to five scintillation vials (20 mL capacity). The vials were capped, placed into a sand bath, and heated in a ramping oven to $100 \text{ }^\circ\text{C}$ at $2.5 \text{ }^\circ\text{C min}^{-1}$, incubated at $100 \text{ }^\circ\text{C}$ for 48 h, and cooled to room temperature at $2.5 \text{ }^\circ\text{C min}^{-1}$. The mother liquor was decanted and the block crystals were rinsed with DMF ($3 \times 10 \text{ mL}$), followed by CHCl_3 (10 mL), and left to soak overnight. After 24 h, the CHCl_3 was decanted and fresh CHCl_3 was added. This was repeated two more times for a total of 3 days of soaking in CHCl_3 . Yield: IRMOF-1-L1 ($\text{Zn}_4\text{O}(\text{C}_{15}\text{H}_9\text{NO}_7)_3$, FW = $1223.2 \text{ g mol}^{-1}$) 45 mg (0.036 mmol, 11%); IRMOF-1-L2 ($\text{Zn}_4\text{O}(\text{C}_{17}\text{H}_{13}\text{NO}_9)_3$, FW = $1403.4 \text{ g mol}^{-1}$) 32 mg (0.023 mmol, 7%).

IRMOF-1-(L1)(NH₂)

IRMOF-1-(L1)(NH₂) was synthesized by employing the same reaction conditions as stated above and using $\text{Zn}(\text{NO}_3)_2 \cdot 6\text{H}_2\text{O}$ (832 mg, 2.8 mmol), L1 (602 mg, 1.9 mmol), and 2-aminoterephthalic acid (NH₂-BDC, 90 mg, 0.5 mmol). Yield: ($\text{Zn}_4\text{O}(\text{C}_{15}\text{H}_9\text{NO}_7)_{2.1}(\text{C}_8\text{H}_5\text{NO}_4)_{0.9}$, FW = $1100.7 \text{ g mol}^{-1}$) 58 mg (0.052 mmol, 9%).

IRMOF-1-(L2)(NH₂)

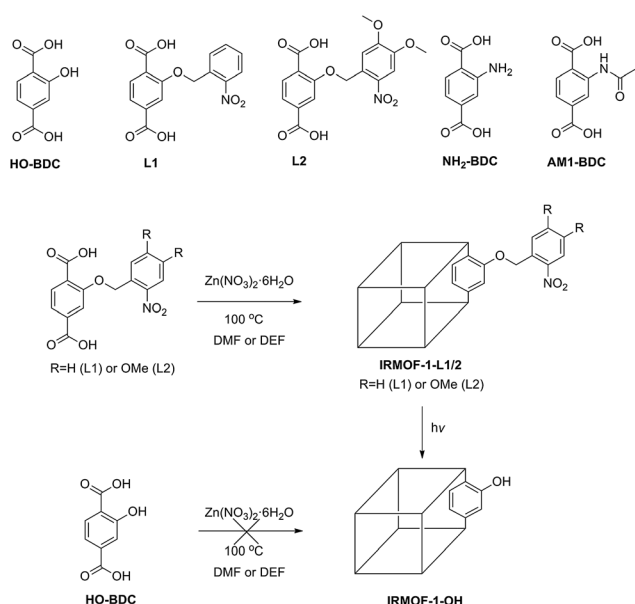
IRMOF-1-(L2)(NH₂) was synthesized by employing the same reaction conditions as stated above and using $\text{Zn}(\text{NO}_3)_2 \cdot 6\text{H}_2\text{O}$ (832 mg, 2.8 mmol), 2-((4,5-dimethoxy-2-nitrobenzyl)oxy)terephthalic acid (377 mg, 1.0 mmol), 2-aminoterephthalic acid (NH₂-BDC, 90 mg, 0.5 mmol). Yield: ($\text{Zn}_4\text{O}(\text{C}_{17}\text{H}_{13}\text{NO}_9)_{1.8}(\text{C}_8\text{H}_5\text{NO}_4)_{1.2}$, FW = $1168.0 \text{ g mol}^{-1}$) 35 mg (0.029 mmol, 7%).

Postsynthetic deprotection

Each vial of crystals was rinsed with EtOAc ($3 \times 10 \text{ mL}$), leaving the crystals stored in 10 mL of EtOAc. The vial was sealed with a screw cap and placed into a Rayonet RPR-200 photoreactor with either 365 nm or 400 nm lamps. Samples were irradiated for a total of 48 h. During irradiation, the crystals were washed with EtOAc ($2 \times 10 \text{ mL}$) three times a day. Upon completion, the crystals were rinsed with EtOAc ($2 \times 10 \text{ mL}$) and exchanged into CHCl_3 ($2 \times 10 \text{ mL}$) until further use.

Postsynthetic modification

IRMOF-1-(L)(AM1), L = L1 or L2. The storage solution from a vial of IRMOF-1-(L1)(NH₂) or IRMOF-1-(L2)(NH₂) was



Scheme 1 Ligand naming system and incorporation of the protected HO-BDC ligands into an IRMOF framework followed by PSD.

decanted and CHCl_3 (5 mL) was added. Acetic anhydride (30 μL , 0.32 mmol) was added, the vial was capped, and the mixture placed into an oven at 55 $^\circ\text{C}$ for 24 h. This process was repeated one more time for IRMOF-1-(L2)(NH_2) for a total reaction time of 48 h. The crystals were rinsed with CHCl_3 (3×10 mL) and left to soak overnight. The crystals were soaked in 10 mL of fresh CHCl_3 for the 2 days, replacing the mother liquor once every day. $\sim 99\%$ yield.

Results and discussion

Synthesis of IRMOFs

We have previously reported the incorporation of the relatively bulky L1 ligand into the UCMCM-1 framework, which is well accommodated by the large pores in this material (14 and 32 \AA).^{12,25} However, we were somewhat surprised to find that both L1 and a dimethoxy analogue L2 could be fully incorporated into an IRMOF lattice with relative ease (11 \AA).^{4,26} Bulky ligands, such as 2,5-bis(benzyloxy)terephthalic acid have been incorporated into an IRMOF, but the degree of incorporation (with BDC as a co-ligands) was limited to $\sim 30\%$, indicative of a steric restriction for bulky groups in the IRMOF lattice.¹³ Combining L1 with $\text{Zn}(\text{NO}_3)_2 \cdot 6\text{H}_2\text{O}$ in *N,N*-dimethylformamide (DMF) or L2 with $\text{Zn}(\text{NO}_3)_2 \cdot 6\text{H}_2\text{O}$ in *N,N*-diethylformamide (DEF) at 100 $^\circ\text{C}$ for 48 h produced cubic colorless or yellow crystals of IRMOF-1-L1 and IRMOF-1-L2, respectively. If DMF was used for the synthesis for IRMOF-1-L2, no crystals were obtained. The IRMOF lattice structure of both materials was directly confirmed by both powder X-ray diffraction (PXRD) and single crystal X-ray diffraction (XRD) techniques (Fig. 1, ESI[†]). XRD structure determination of IRMOF-1-L1 and IRMOF-1-L2 unambiguously resolved the expected IRMOF lattice (ESI[†]). In addition, diffuse electron density was found in the pores of both materials that was suggestive of the nitrobenzyl protecting groups, but the substituents could not be clearly assigned due to severe disorder. The composition of the ligands in these frameworks was verified by other methods.

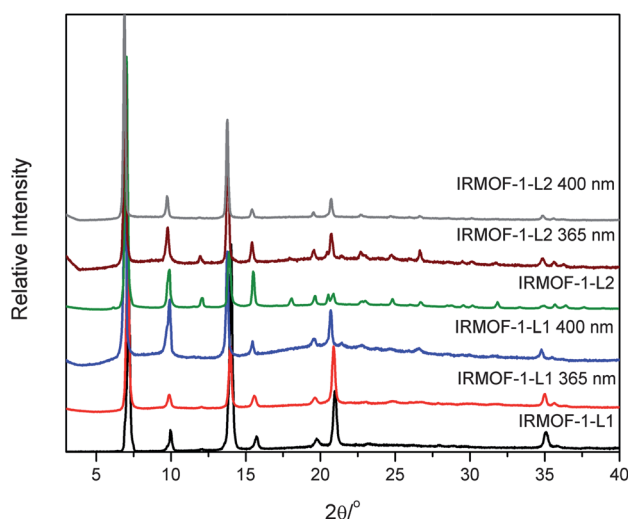


Fig. 1 Powder X-ray diffraction of frameworks before and after PSD.

Thermogravimetric analysis (TGA) of IRMOF-1-L1 displays a sharp weight loss at 260 $^\circ\text{C}$ ($\sim 40\%$) indicative of thermal liberation of the nitrobenzyl group (ESI[†]). IRMOF-1-L2 does not have the same drastic drop, but has a gradual thermal trace that shows MOF degradation ~ 400 $^\circ\text{C}$. Dissolution of IRMOF-1-L1 and IRMOF-1-L2 crystals in acid allowed for analysis of their chemical composition by ^1H NMR spectroscopy and electrospray ionization mass spectrometry (ESI-MS). Both methods showed that ligands L1 and L2 were successfully incorporated into the IRMOFs without degradation or loss of the protecting group (Fig. 2). BET surface area measurements with dinitrogen at 77 K gave values of 1407 $\text{m}^2 \text{g}^{-1}$ and 1164 $\text{m}^2 \text{g}^{-1}$ for IRMOF-1-L1 and IRMOF-1-L2, respectively (Table 1). Although these surface area values are lower than that of many other IRMOFs,⁴ they are consistent with the introduction of the large nitrobenzyl groups into the framework pores.

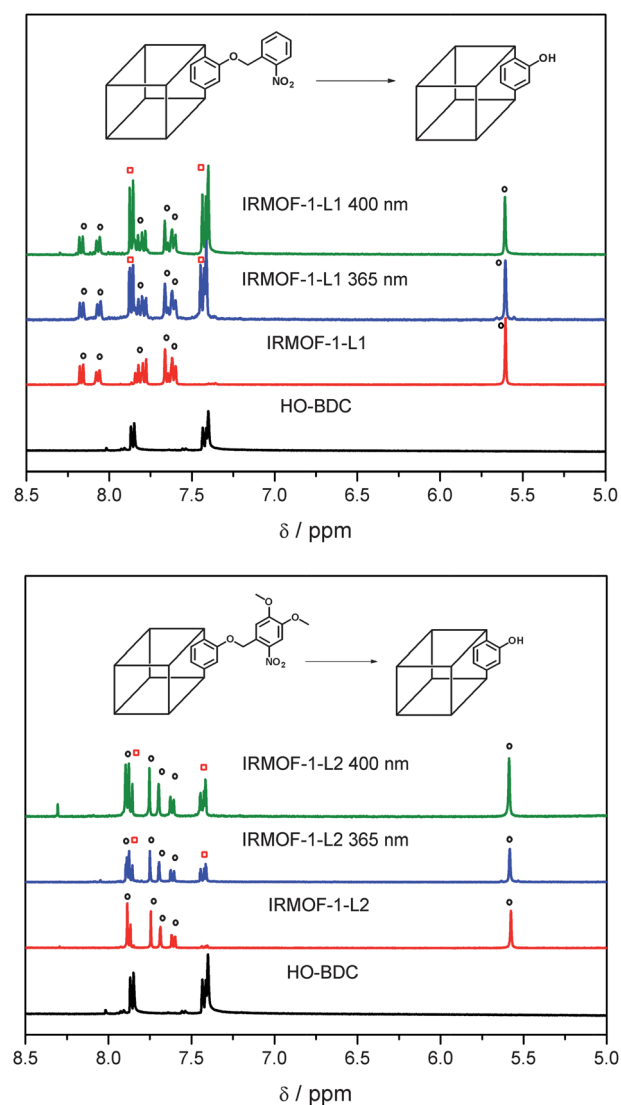


Fig. 2 ^1H NMR of digested samples of IRMOF before and after PSD at both 365 nm and 400 nm wavelengths. Starting materials are marked with black circles and the product is marked by red squares. A ^1H NMR for an authentic sample of HO-BDC is provided as a reference.

Table 1 BET surface areas for the IRMOFs. Percent deprotection (% PSD) based on ^1H NMR spectroscopic analysis of samples digested in d^6 -DMSO/ $\text{DCI}/\text{D}_2\text{O}$ solution after irradiation at either 365 or 400 nm. The standard deviation for all reported BET values is no more than $\pm 150 \text{ m}^2 \text{ g}^{-1}$

MOF	BET ($\text{m}^2 \text{ g}^{-1}$)	% PSD 365 nm	% PSD 400 nm
IRMOF-1-L1	1407	80 (2344 $\text{m}^2 \text{ g}^{-1}$)	83
IRMOF-1-L2	1164	53	58
IRMOF-1-(L1)(NH_2)	1584	<10	42
IRMOF-1-(L2)(NH_2)	1615	33	40
IRMOF-1-(L1)(AM1)	1427	53	63
IRMOF-1-(L2)(AM1)	1344	70	77

Postsynthetic deprotection of IRMOFs

IRMOF-1-L1 and IRMOF-1-L2 were irradiated in a photochemical reactor at one of two wavelengths, 365 or 400 nm, for 48 h to effect PSD of the materials and obtain IRMOFs with phenolic groups in the pores. The percent conversion of the PSD reaction was determined using ^1H NMR after digesting the materials in acid (Fig. 2). IRMOF-1-L1 gave 80–83% conversion to IRMOF-1-OH whether irradiated at either 365 nm or 400 nm (Table 1). A concomitant increase in BET surface area, as observed in our previous studies,¹² was found for the product IRMOF-1-OH, showing an average BET value of $\sim 2344 \text{ m}^2 \text{ g}^{-1}$ (Fig. 3, Table 1). IRMOF-1-L2 also did not show a substantial difference in PSD efficiency as a function of wavelength, giving between 53–58% conversion to IRMOF-1-OH whether irradiated at 365 or 400 nm (Fig. 2). A steric effect may be contributing to this slow deprotection of IRMOF-1-L2, as the pores of this IRMOF are more restricted than IRMOF-1-L1 due to the additional methoxy groups on the protecting group. The dimethoxynitrosobenzaldehyde byproduct of the photochemical reaction may be more strongly retained in the pores and further interfere with the PSD reaction, due to the large extinction coefficient of dimethoxynitrosobenzaldehyde.²⁷ However, we find little evidence that these aldehyde byproducts remain in the

framework (based on NMR and ESI-MS analysis of the final MOF products). All samples showed little to no change in the PXRD patterns (Fig. 1) after irradiation, confirming the pristine nature of the crystals. Preservation of crystallinity was also readily apparent by visual inspection, where only a color change was observed, but the crystals appeared otherwise undisturbed as confirmed through single crystal XRD (ESI†).

Changing the electronics of the nitrobenzyl group is a common tactic used to shift the absorption wavelength for photocleavage. Based on previous reports,¹⁹ it was expected that the nitrobenzyl group (L1) would cleave with a λ_{max} at 365 nm, while the dimethoxy derivative (L2) would cleave more effectively at 400 nm; however, in the MOFs the expected trend was not observed. Also, quantitative deprotection, as was seen in the UCMC system,¹² was not achieved in these IRMOF materials, despite screening a variety of reaction conditions. The differences between the expected photochemical behaviour and our observations here may be due to a number of factors. As will be discussed below, we believe a combination of light absorption and scattering by the IRMOF explains, in part, the attenuation of the photochemical reactions. Both absorption and scattering diminish the amount of light that penetrates through the framework and thus impedes PSD.

Combining PSD and PSM on IRMOFs

Mixed ligand approaches have been utilized to prepare highly functionalized MOF materials.^{14,18} Functional groups that can be introduced presynthetically can serve as chemical handles for PSM. In a recent study from our group, we investigated tandem PSM on a mixed ligand system. Two different BDC ligands, NH_2 -BDC and Br-BDC, were incorporated into a UiO-66 framework and modified orthogonally *via* PSM.^{15,28} In this case, the order in which the orthogonal PSM reactions were performed (*i.e.* PSM of NH_2 -BDC before Br-BDC *versus* PSM of Br-BDC then NH_2 -BDC) had no effect on the overall yields. Hence the PSM reactions could be performed in any order, allowing for the preparation of several bifunctional MOFs.¹⁵

In order to investigate the possibility of performing tandem PSD-PSM, NH_2 -BDC was chosen as the co-ligand to make mixed IRMOFs. Upon mixing L1 and NH_2 -BDC in a 3.8 : 1 ratio with $\text{Zn}(\text{NO}_3)_2$ in DEF at 100 °C for 48 h, amber-colored crystals of IRMOF-1-(L1)(NH_2) were obtained. The 3.8 : 1 ligand ratio gave the highest quality crystals based on visual inspection and PXRD analysis (data not shown) from a screening of a large number of ligand ratios and reaction conditions. ^1H NMR spectroscopy of the digested crystals indicate that NH_2 -BDC comprised $\sim 30\%$ of the ligands of this IRMOF. PXRD and single crystal XRD confirmed that IRMOF-1-(L1)(NH_2) possessed the correct topology, although the BDC substituents could not be assigned in the difference map. The BET surface area of IRMOF-1-(L1)(NH_2) was $\sim 1584 \text{ m}^2 \text{ g}^{-1}$, higher than IRMOF-1-L1, which is consistent with the smaller NH_2 -BDC ligand being incorporated (Table 1). Using similar conditions for L2 and NH_2 -BDC in a 2 : 1 ratio, amber blocks were obtained with $\sim 40\%$ NH_2 -BDC incorporation. The more efficient incorporation of NH_2 -BDC into IRMOF-1-(L1)(NH_2) and IRMOF-1-(L2)(NH_2) is attributed the greater solubility of NH_2 -BDC when compared to L1 and L2. It is also

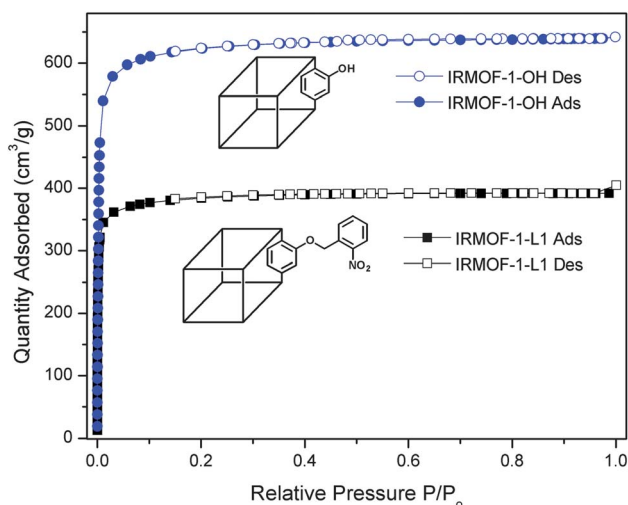
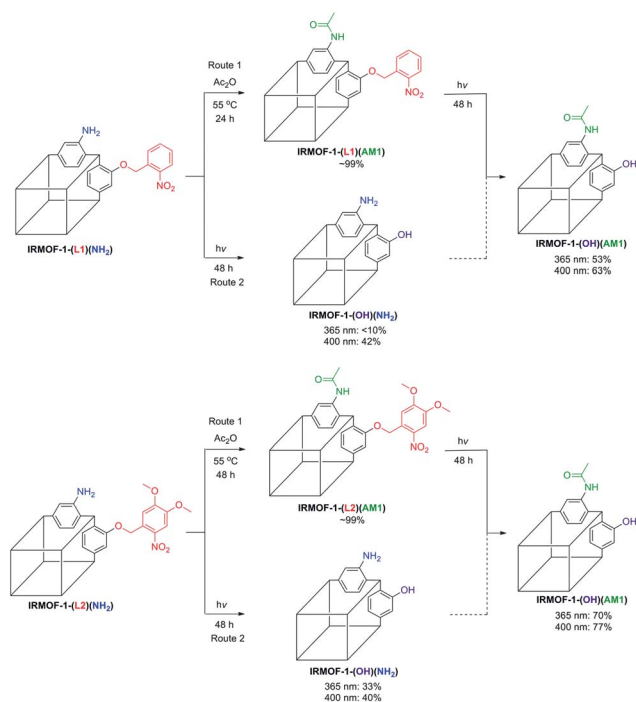


Fig. 3 N_2 adsorption and desorption isotherms for IRMOF-1-L1 and IRMOF-1-OH generated by PSD using 365 nm light.

possible that steric factors, L1 and L2 being much more bulky, play a role in the differences observed with respect to ligand incorporation and the overall low yields of IRMOF formation. IRMOF-1-(L2)(NH₂) gave a BET value $\sim 1615 \text{ m}^2 \text{ g}^{-1}$, understandably due to the larger L2 ligand, and a higher percentage of NH₂-BDC (Table 1). Analogous to the orthogonal PSM mentioned previously,¹⁵ we explored two routes for tandem PSD-PSM: PSM followed by PSD (route 1), and PSD followed by PSM (route 2) (Scheme 2). These two routes were evaluated based on the best combination of percent PSM, percent PSD, and crystallinity of the final materials. It is worth noting that, like our previous study on tandem PSM,¹⁵ this methodology potentially leads to two intermediate and a final MOF from each starting framework.

Using route 1, where PSM is performed before PSD, we found both IRMOF-1-(L1)(NH₂) and IRMOF-1-(L2)(NH₂) were quantitatively transformed to the acetamide IRMOF-1-(L1)(AM1) and IRMOF-1-(L2)(AM1), respectively. After PSM, PSD on IRMOF-1-(L1)(AM1) gave ~ 53 – 63% PSD at 365 or 400 nm (Table 1, Fig. 4). This is markedly lower than the photocleavage of IRMOF-1-L1 at either wavelength. Crushing the crystals gave only modest increases in the PSD yields of mixed IRMOFs (10–15%). However, IRMOF-1-(L2)(AM1) gave ~ 70 – 77% PSD at 365 or 400 nm, which is an improved yield when compared to IRMOF-1-L2. Unfortunately, we were unable to identify reaction conditions where PSD in these IRMOFs would go to completion. Nonetheless, for route 1 it was found that L2 was a better group for PSD at both wavelengths.

Route 2, where PSD was performed prior to PSM, gave less impressive results than route 1. Photolysis of IRMOF-1-(L1)(NH₂), at 365 nm shows minimal ($<10\%$) PSD (Table 1, Fig. 4).



Scheme 2 Tandem PSD-PSM routes for functionalization of mixed ligand IRMOFs. Yields are based on ¹H NMR spectroscopic analysis of samples digested in *d*⁶-DMSO/DCI/D₂O solution.

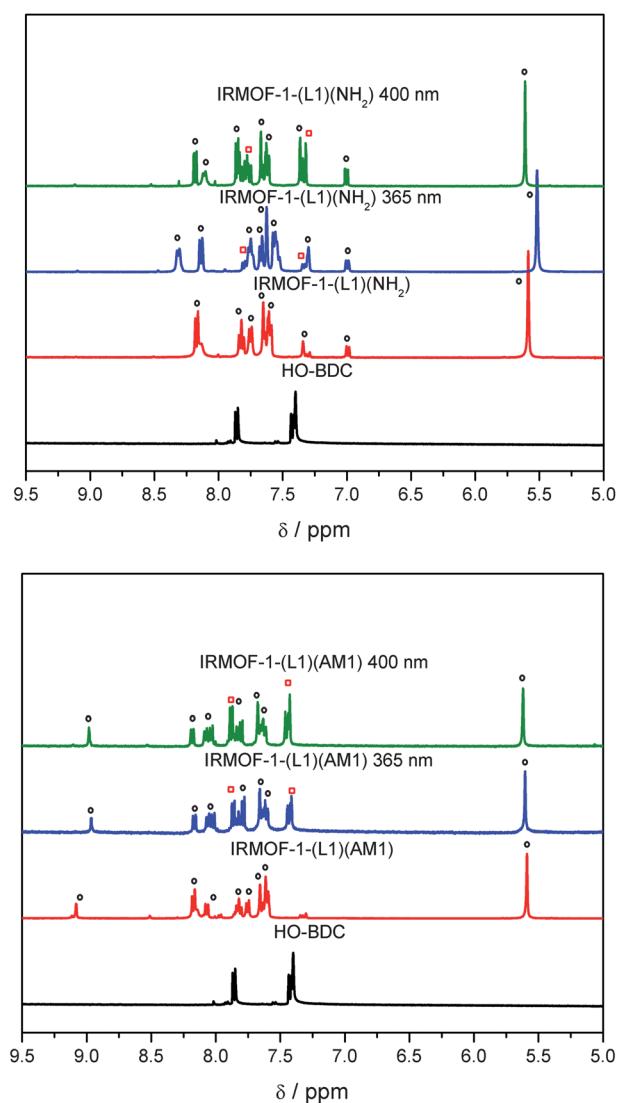


Fig. 4 ¹H NMR of digested IRMOF-1-(L1)(AM1) (top, route 1) and IRMOF-1-(L1)(NH₂) (bottom, route 2) before and after PSD at 365 nm or 400 nm. Starting materials are marked with black circles and the product is marked by red squares. A ¹H NMR for an authentic sample of HO-BDC is provided as a reference.

The reason for this low yield is discussed in detail below. At 400 nm, 42% PSD was observed, which is much lower than the 83% PSD observed for IRMOF-1-L1. Interestingly, IRMOF-1-(L2)(NH₂) shows 33% and 40% deprotection at 365 nm and 400 nm, respectively (ESI†). This correlates better with the 53% and 58% PSD obtained with IRMOF-1-L2 at the same wavelengths. However, due to the generally lower than desired PSD results, route 2 was not further explored. Overall, it appears route 1 gives better PSD conversions than route 2. Unlike our previous study on tandem PSM, the order of PSD *versus* PSM was important for obtaining the desired materials.¹⁵

In order to understand the poor PSD at 365 nm for IRMOF-1-(L1)(NH₂), the absorption spectra of the homogeneous, free ligand systems were examined. UV-Vis spectroscopy studies on the methyl diester forms of the ligands provided some insight into

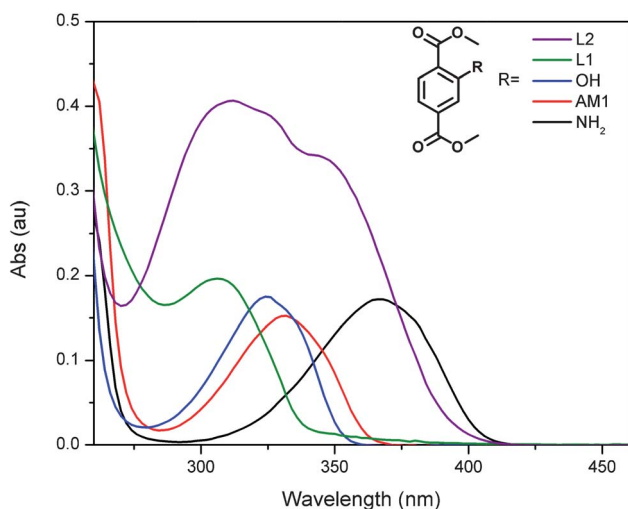


Fig. 5 UV-Visible absorption spectra of the methyl diester form of several ligands (50 μM) in EtOAc.

the failure of these PSD reactions (Fig. 5). Photocleavage of 2-nitrobenzyl groups has been well studied with the near-UV range (300–400 nm) providing the optimal wavelengths for promotion of this reaction.¹⁹ The λ_{max} for the methyl diesters forms of L1, $\text{NH}_2\text{-BDC}$, AM1-BDC, and HO-BDC were 310, 368, 330, and 325 nm, respectively (Fig. 5). This strongly indicates that the reduced PSD of L1 in IRMOF-1-(L1)(NH_2) can be attributed to the strong absorption by the $\text{NH}_2\text{-BDC}$ ligands compared to L1 at 365 nm. Based on this hypothesis, the solution spectra in Fig. 5 suggest that the addition of the methoxy groups in L2 should alter the PSD behaviour in IRMOF-1-(L2)(NH_2) as observed (*vide supra*). Previous reports indicate that the addition of methoxy substituents allows photocleavage at wavelengths up to 420 nm.²³ The broad and very intense absorption of L2 from 300–400 nm drastically increase the efficiency of L2 to absorb at 365 nm thus rendering the observed PSD in the presence of $\text{NH}_2\text{-BDC}$ much more efficient.

The solution UV-Vis spectroscopy also assisted in our understanding of the more effective PSD achieved when using route 1. Acetylation of the amine group to give IRMOF-1-(L1) (AM1) blue-shifts the λ_{max} to 330 nm, thus reducing the interfering absorption at 365 nm and enhancing PSD. Additionally, IRMOF-1-(L2)(AM1) deprotects most out of all the mixed MOFs studied presumably due to a combination of the wide absorbing L2 and the now unobtrusive AM1. This conclusion is loosely supported by the solid-state UV-Vis spectra of the corresponding IRMOFs (ESI†).

Conclusion

We have successfully incorporated two bulky BDC ligands into an IRMOF lattice. L1 and L2 have the same HO-BDC ligand protected with a photolabile group; 2-nitrobenzyl (L1) or 4,5-dimethoxy-2-nitrobenzyl (L2). These groups are known to easily cleave upon exposure to near-UV light and the differences in electronics should alter the deprotection as a function of wavelength used. The IRMOFs prepared from these ligands were irradiated at either 365 or 400 nm to induce PSD of the

framework. IRMOF-1-L1 was found to photodeprotect to IRMOF-1-OH more effectively than IRMOF-1-L2 at both wavelengths.

Recently, multi-functionalized materials have been heavily studied because of their distinct and interesting characteristics in comparison to monofunctional MOFs. To prepare multifunctional MOFs, L1 and L2 were combined with $\text{NH}_2\text{-BDC}$ to produce IRMOF-1-(L1)(NH_2) and IRMOF-1-(L2)(NH_2), respectively. It was found that performing PSM prior to PSD was preferred, due to the strong absorption of the $\text{NH}_2\text{-BDC}$ ligand, which interfered with the PSD reaction. Unlike the ester form of $\text{NH}_2\text{-BDC}$, which photodegrades in solution, the $\text{NH}_2\text{-BDC}$ ligand was persistent in the IRMOF, which only served to further interfere with PSD reaction. These findings indicated that the reaction order in this PSD-PSM combination was an important consideration to achieve good conversions to the desired materials.

In summary, we have studied the heterogeneous PSD of nitrobenzyl protected MOFs in comparison to the homogeneous systems. The utility of multiple postsynthetic approaches (PSD and PSM) on a single, bifunctional MOFs has been demonstrated. The ability to combine pre- and various post-synthetic methods is a key step in obtained highly tailorable materials for technological applications. Related studies, including other postsynthetic photochemical processes are being investigated and will be reported in due course.

Acknowledgements

We thank Dr Min Kim for helpful discussions, Dr Y. Su (U.C.S.D.) for performing mass spectrometry experiments, and Dr C. Moore, Prof. A. Rheingold (U.C.S.D.), and Phuong Dau for assistance with single-crystal X-ray structures. This research was supported by a grant from the National Science Foundation (CHE-0952370). This material is based upon work supported by the National Science Foundation Graduate Research Fellowship (C.A.A.) under Grant No. DGE1144086.

Notes and references

- G. Ferey, *Chem. Soc. Rev.*, 2008, **37**, 191–214.
- J. L. C. Rowsell and O. M. Yaghi, *Microporous Mesoporous Mater.*, 2004, **73**, 3–14.
- H. Li, M. Eddaoudi, M. O’Keeffe and O. M. Yaghi, *Nature*, 1999, **402**, 276–279.
- M. Eddaoudi, J. Kim, N. Rosi, D. Vodak, J. Wachter, M. O’Keeffe and O. M. Yaghi, *Science*, 2002, **295**, 469–472.
- Z. Wang and S. M. Cohen, *Chem. Soc. Rev.*, 2009, **38**, 1315–1329.
- S. M. Cohen, *Chem. Sci.*, 2010, **1**, 32–36.
- K. K. Tanabe and S. M. Cohen, *Chem. Soc. Rev.*, 2011, **40**, 498–519.
- S. Bernt, V. Guillerme, C. Serre and N. Stock, *Chem. Commun.*, 2011, **47**, 2838–2840.
- T. Gadzikwa, O. K. Farha, C. D. Malliakas, M. G. Kanatzidis, J. T. Hupp and S. T. Nguyen, *J. Am. Chem. Soc.*, 2009, **131**, 13613–13615.
- R. K. Deshpande, G. I. N. Waterhouse, G. B. Jameson and S. G. Telfer, *Chem. Commun.*, 2012, DOI: 10.1039/C1CC12884A.
- R. K. Deshpande, J. L. Minnaar and S. G. Telfer, *Angew. Chem., Int. Ed.*, 2010, **49**, 4598–4602.
- K. K. Tanabe, C. A. Allen and S. M. Cohen, *Angew. Chem., Int. Ed.*, 2010, **49**, 9730–9733.
- H. Deng, C. J. Doonan, H. Furukawa, R. B. Ferreira, J. Towne, C. B. Knobler, B. Wang and O. M. Yaghi, *Science*, 2010, **327**, 846–850.

- 14 A. D. Burrows, *CrystEngComm*, 2011, **13**, 3623–3642.
- 15 M. Kim, J. F. Cahill, K. A. Prather and S. M. Cohen, *Chem. Commun.*, 2011, **47**, 7629–7631.
- 16 A. D. Burrows, L. C. Fisher, C. Richardson and S. P. Rigby, *Chem. Commun.*, 2011, **47**, 3380–3382.
- 17 S. Marx, W. Kleist, J. Huang, M. Maciejewski and A. Baiker, *Dalton Trans.*, 2010, **39**, 3795–3798.
- 18 T. Lescouet, E. Kockrick, G. Bergeret, M. Pera-Titus and D. Farrusseng, *Dalton Trans.*, 2011, **40**, 11359–11361.
- 19 J. A. Mccray and D. R. Trentham, *Annu. Rev. Biophys. Biophys. Chem.*, 1989, **18**, 239–270.
- 20 C. G. Bochet, *Tetrahedron Lett.*, 2000, **41**, 6341–6346.
- 21 G. Mayer and A. Heckel, *Angew. Chem., Int. Ed.*, 2006, **45**, 4900–4921.
- 22 H. Sato, R. Matsuda, K. Sugimoto, M. Takata and S. Kitagawa, *Nat. Mater.*, 2010, **9**, 661–666.
- 23 A. Albin and M. Fagnoni, *Handbook of synthetic photochemistry*, Wiley-VCH, Weinheim, 2010.
- 24 A. J. Blake, N. R. Champness, T. L. Easun, D. R. Allan, H. Nowell, M. W. George, J. Jia and X.-Z. Sun, *Nat. Chem.*, 2010, **2**, 688–694.
- 25 K. Koh, A. G. Wong-Foy and A. J. Matzger, *Angew. Chem., Int. Ed.*, 2008, **47**, 677–680.
- 26 Z. Wang and S. M. Cohen, *J. Am. Chem. Soc.*, 2007, **129**, 12368–12369.
- 27 M. Gaplovsky, Y. V. Il'ichev, Y. Kamdzhilov, S. V. Kombarova, M. Mac, M. A. Schworer and J. Wirz, *Photochem. Photobiol. Sci.*, 2005, **4**, 33–42.
- 28 J. H. Cavka, S. Jakobsen, U. Olsbye, N. Guillou, C. Lamberti, S. Bordiga and K. P. Lillerud, *J. Am. Chem. Soc.*, 2008, **130**, 13850–13851.